Targeted Alpha Therapy

Subjects: Pharmacology & Pharmacy

Contributor: Frank Wuest, Bryce Nelson

This article discusses the therapeutic advantages of Targeted Alpha Therapy (TAT), including the short and highly ionizing path of α-particle emissions; the ability of TAT to complement and provide superior efficacy over existing forms of radiotherapy; and the physical decay properties and radiochemistry of common α-emitters, including ^{225}Ac, ^{213}Bi, ^{224}Ra, ^{212}Pb, ^{227}Th, ^{223}Ra, ^{211}At.

Keywords: targeted alpha therapy ; alpha particle therapy ; actinium-225 ; terbium-149 ; radium-223 ; astatine-211 ; bismuth-213 ; thorium-227 ; radium-224 ; radiotherapy

1. Introduction

Radionuclide therapy has been employed frequently in the past several decades for disease control, curative therapy, and pain management applications [1]. Targeted radionuclide therapy (TRT) is advantageous as it delivers a highly concentrated dose to a tumor site—either directly to the tumor cells or to its microenvironment—while sparing the healthy surrounding tissues. It has been clinically demonstrated using a variety of radionuclides to treat malignancies, including polycythemia, cystic craniopharyngioma, hyperthyroidism, synovitis and arthritis, and numerous cancers, such as thyroid cancer, bone tumors and metastasis, hepatic metastasis, ovarian cancer, neuroendocrine tumors, leukemia, lymphoma, and metastatic prostate cancer [2][3][4]. Since radionuclide therapy targets diseases at the cellular level, it has advantages for treating systemic malignancies such as tumor metastases over other forms of therapy such as external beam therapy, where full body irradiation is impossible. In addition to being minimally invasive, radionuclide therapy can be shorter in duration than chemotherapy [2].

In TRT, therapeutic radionuclides including alpha (α), beta (β^-), and Auger electron emitters are typically conjugated to a targeting vector such as monoclonal antibodies, biomolecules, peptides, nanocarriers, and small-molecule inhibitors. To maximize the therapeutic efficacy of a TRT radiopharmaceutical, its radionuclide decay pathway, particle emission range, and relative biological effectiveness should be matched appropriately for a given tumor mass, size, radiosensitivity, and heterogeneity [1].

This review focuses on targeted alpha therapy (TAT), outlined by the graphical abstract in Figure 1. A detailed overview of α-emitting radionuclides currently employed in radiotherapy is presented and compared to radionuclides with different emissions, including β^- particle and auger electron emitters. Production techniques for α-emitters are outlined, including their separation and unique handling requirements, followed by their radiochemistry and targeting characteristics. Preclinical developments and clinical applications of α-emitters are discussed along with current limitations, potential areas for improvement, and anticipated applications.

Figure 1. Key aspects of targeted alpha therapy: (**a**) radionuclide production via cyclotron, nuclear reactor or generator decay, and shielded automated processing; (**b**) radiolabeling the alpha-emitting radionuclide to a suitable targeting vector to form a bioconjugate; and (**c**) targeted alpha radiotherapy precisely destroys tumor cells while sparing surrounding healthy tissue.

2. Selecting Radionuclides for Radiotherapy

When selecting a radionuclide for clinical application, the physical and biochemical characteristics must be considered. Physical characteristics include physical half-life, type of emissions, energy of the emissions, daughter products, method of production, and radionuclidic purity. Biochemical characteristics include tissue targeting, retention of radioactivity in the tumor, in vivo stability, and toxicity [2]. For radiotherapy, it is desirable to have a high linear energy transfer (LET), where there is a high ionization energy deposited per unit length of travel. Radionuclides with a high LET deposit radioactive emission energy within a small range of tissue, thereby sparing surrounding healthy tissue and keeping the radioactive dose within, as much as possible, the patient's organ to be treated. It can also be advantageous for the therapeutic radionuclide, or a complementary theranostic radionuclide, to emit positrons (β^+) or gamma (γ) radiation. This enables positron emission tomography (PET) or single photon emission tomography (SPECT) imaging and visualization of radiopharmaceutical distribution within a patient's body, permitting treatment monitoring. Table 1 outlines key characteristics of α, β^-, and auger electron emitters, and some clinical applications for cancer TRT that have been explored.

Table 1. Key characteristics of α, β^-, and auger electron emitters and their clinical applications.

Radioactive Particle	Decay Characteristics	Clinical Cancer Applications	Reference
Beta particle (β^-)	Emission energy per decay: 50–2300 keV Range: 0.05–12 mm Linear Energy Transfer (LET**):** 0.2 keV/µm	Metastatic castration resistant prostate cancer, acute myeloid leukemia, neuroendocrine tumors, acute lymphocytic leukemia, ovarian carcinomas, gliomas, metastatic melanoma, colon cancer, bone metastases	[1][3][4]
Auger electron (AE)	Emission energy per decay: 0.2–200 keV Range: 2–500 nm LET: 4–26 keV/µm	Advanced pancreatic cancer with resistant neoplastic meningitis, advanced sst-2 positive neuroendocrine and liver malignancies, metastatic epidermal growth factor receptor (EGFR)-positive breast cancer, glioblastoma multiforme	[1][5]
Alpha particle (α)	Emission energy per decay: 5–9 MeV Range: 40–100 µm LET: 80 keV/µm	Metastatic castration resistant prostate cancer, relapsed or refractory CD-22-positive non-Hodgkin lymphoma, acute myeloid leukemia, neuroendocrine tumors, ovarian carcinoma, gliomas, intralesional and systemic melanoma, colon cancer, bone metastases	[1][3][4]

β^- emitting radioisotopes have a relatively long pathlength (≤12 mm) and a lower LET of ~0.2 keV/µm, giving them effectiveness in medium–large tumors [1]. However, they lack success in solid cancers with microscopic tumor burden. This may be attributed to their emissions releasing the majority of their energy along a several millimeter long electron track, irradiating the surrounding healthy tissue instead of depositing their main energy into the micro-metastatic tumor cells where the radionuclide was delivered [6].

Clinical success has been demonstrated with the β^- emitters ^{90}Y and ^{131}I conjugated with anti-CD20 monoclonal antibodies in follicular B-cell non-Hodgkin lymphoma [6], ^{177}Lu-labeled prostate-specific membrane antigen (PSMA) peptides in metastatic, castration-resistant prostate cancer (CRPC) and ^{177}Lu-DOTATATE for neuroendocrine tumors [7][8].

Auger electrons have a medium LET (4–26 keV/μm) [1]; however, their short pathlength of 2–500 nm limits the majority of their effects to within single cells, requiring the radionuclide to be transported into the cell and preferably incorporated into DNA to achieve high lethality. They can also kill cancer cells by damaging the cell membrane and kill non-directly targeted cells through a cross-dose or bystander effect [9]. Clinical studies with Auger electrons for cancer therapy have been limited; however, some encouraging results were obtained using [^{111}In]In-DTPA-octreotide in rats with pancreatic tumors, [^{125}I]I-IUdR where tumor remissions were achieved, and [^{125}I]I-mAb 425 where the survival of glioblastoma patients improved [5][10][11]. However, it has also been determined that some Auger electron emitting compounds, such as [^{123}I]I-IUdR and [^{125}I]I-IUdR only kill cells in the S-phase of the cell cycle, highlighting a potential treatment limitation [12].

α-particles have a high LET (80 keV/μm) and a moderate pathlength (50–100 μm), giving them an effective range of less than 10 cell diameters. This makes them suitable for microscopic tumor cell clusters, while sparing normal organs and surrounding healthy tissues. Importantly, α-particle lethality is not dependent on the cell cycle or oxygenation, and the DNA damage is often via double strand and DNA cluster breaks and is therefore much more difficult to repair than β^- damage [6]. It has been estimated that to attain a single cell kill probability of 99.99%, tens of thousands of β^- decays are required, whereas only a few α-decays at the cell membrane achieves the same kill probability [13]. From this, it has been estimated that one α particle transversal can kill a cell [14]. Most α-emitters are conjugated to a wide range of targeting vectors for delivery to their target site, though some have intrinsic targeting properties, such as the affinity of ^{223}Ra-dichloride for bone [1]. Preclinical and clinical studies using α-emitters have been ongoing for a variety of cancers, some of which include recurrent brain tumors, recurrent ovarian cancers, human epidermal growth factor receptor-2 (HER-2) positive cancers, myelogenous leukemia, non-Hodgkin lymphoma, metastatic melanoma, and skeletal metastases in prostate cancer [6]. Of these, the most theranostic research is performed on prostate and neuroendocrine tumors (NETs). Examples of studies are numerous—one preclinical study using [^{212}Pb]Pb-trastuzumab found a single injection reduced tumor growth by 60–80%, reduced aortic lymph node metastasis, and prolonged survival or tumor-bearing mice [15]. Another study outlined how α-particle radiotherapy for metastatic castration resistant prostate cancer using [^{225}Ac]Ac-PSMA-617 was able to overcome resistance to [^{177}Lu]Lu-PSMA-617 β^--particle therapy [16]. Additionally, a study using [^{213}Bi]Bi-DTPA and [^{213}Bi]Bi-DOTATATE in mice resulted in a factor of six increase in cell killing compared to [^{177}Lu]Lu-DOTATATE [17][18]. These studies highlight the clinical importance and potential of α-emitters, and their potential to be more efficient and effective than β^-- therapy.

3. Alpha Emitter Decay Properties

As emissions from radioactive decay, α-particles are naked ^{4}He nuclei with a +2 charge. They are 7300 times larger than the mass of β^- and Auger electrons, giving them significant emission momentum that reduces deflection and results in a near-linear emission path, as opposed to the winding path of β^- particles. With an emission kinetic energy between 5–9 MeV, coupled with a particle range of 50–100 μm, this classifies α-particles as high LET. The energy distribution between the alpha particle and the recoiling daughter atom is typically 98% to 2%. Upon decay, energy imparted to the daughter recoil atom can reach 100 keV [19], which is far higher than the binding energy of the strongest chemical bonds, resulting in release of the daughter isotope from its targeting vector. An example is ^{219}Rn, which has a daughter recoil range of 88 nm in a cellular environment [19]. These daughters often have a serial decay chain with their own α-emitting progeny, leading to untargeted irradiation of surrounding tissues. As a result, only a limited number of α-emitting radioisotopes are suitable for therapy due to their decay characteristics. The half-life of the radionuclide should be reasonable for therapy; it should not be too short to allow sufficient time for production, radiopharmaceutical synthesis, and delivery to the patient, and it, as well as the half-life of any daughter radionuclide, should not be too long to avoid excess patient dose.

The recoil energy caused by the decay of α-emitters invariably destroys α-emitter-targeting vector chemical bonds, often releasing α-emitting progeny with different chemistries that can lead to undesirable toxicities. The presence of γ-ray emissions in an α-emitter decay chain is also of interest for imaging purposes. Therefore, it is important to understand the half-lives, emissions, and decay characteristics when selecting clinically relevant α-emitters. Figure 2 depicts decay chains that contain some common therapeutic α-emitters, and Table 2 outlines the decay characteristics of some notable α-emitters used in α therapy, including their daughters, half-lives, decay energies, and emissions.

Table 2. Notable α-emitters and their daughters, half-lives, decay energies, and emission types [20].

			Emission Type (Energy, Intensity)				
Parent	**Daughters**	**Half-Life**					
			α	**β^-**	**β^+**	**γ**	**X-Ray**

^{225}Ac		9.9 d	5.8 MeV, 50.7%		100 keV, 1%	18.6 keV, 13%
	^{221}Fr	4.8 min	6.3 MeV, 83.3%		218 keV, 11.4%	17.5 keV, 2%
	^{217}At	32.3 ms	7.1 MeV, 99.9%			
	^{213}Bi	45.6 min	5.9 MeV, 1.9%	492 keV, 66%	440 keV, 26%	79 keV, 1.8%
	^{213}Po	3.72 μs	8.4 MeV, 100%			
	^{209}Tl	2.16 min		178 keV, 0.4%	1567 keV, 99.7%	75 keV, 9.7%
	^{209}Pb	3.23 h		198 keV, 100%		
	^{209}Bi	Stable				
^{224}Ra		3.63 d	5.7 MeV, 95%		241 keV, 4.1%	
	^{220}Rn	55.6 s	6.3 MeV, 99.9%			
	^{216}Po	0.15 s	6.8 MeV, 99.9%			
	^{212}Pb	10.6 h		93.5 keV, 83%	238 keV, 43.6%	77 keV, 17.5%
	^{212}Bi	60.6 min	6.1 MeV, 25%	834 keV, 55%	727 keV, 6.7%	15 keV, 7%
	^{212}Po	0.30 μs	8.8 MeV, 100%			
	^{208}Tl	3.1 min		650 keV, 49%	2614 keV, 99.9%	
	^{208}Pb	Stable				

^{227}Th		18.7 d	6.0 MeV, 100%			236 keV, 13%	19 keV, 37%
	^{223}Ra	11.4 d	5.7 MeV, 100%			269 keV, 14%	83 keV, 25%
	^{219}Rn	3.96 s	6.8 MeV, 79.4%			271 keV, 10%	16 keV, 1%
	^{215}Po	1.78 ms	7.4 MeV, 99.9%				
	^{211}Pb	36.1 min		471 keV, 91%		404 keV, 3.8%	
	^{211}Bi	2.14 min	6.6 MeV, 83.5%	172 keV, 0.3%		351 keV, 13%	
	^{207}Tl	4.77 min		492 keV, 99.7%			
	^{207}Pb	Stable					
^{211}At		7.2 h	5.9 MeV, 42%				79 keV, 21%
	^{211}Po	0.52 s	7.5 MeV, 98.9%				
	^{207}Bi	31.6 y				570 keV, 97.8%	
	^{207}Pb	Stable					
^{149}Tb		4.1 h	4.0 MeV, 16.7%		638 keV, 3.8%	352 keV, 29.4%	43 keV, 36%
	^{149}Gd	9.3 d				150 keV, 48%	42 keV, 55%
	^{149}Eu	93.1 d					40 keV, 40%
	^{149}Sm	Stable					
	^{145}Eu	5.9 d			740 keV, 1.5%	894 keV, 66%	40 keV, 40%

^{145}Sm	340.3 d	61 keV, 12%	39 keV, 71%
^{145}Pm	17.7 y	72 keV, 2%	37 keV, 40%
^{145}Nd	Stable		

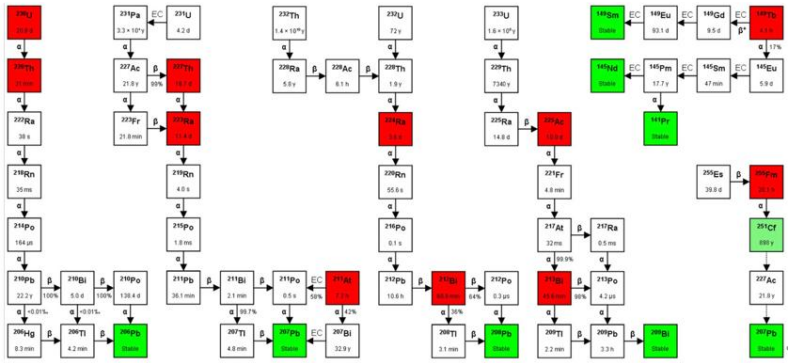

Figure 2. Decay chains of some common therapeutic α-emitters [6].

^{225}Ac ($t_{1/2}$ = 9.9 d, 5.8 MeV α particle) decays to ^{209}Bi with six intermediate radionuclide progenies. These daughters include ^{221}Fr ($t_{1/2}$ = 4.8 min; 6.3 MeV α particle and 218 keV γ emission), ^{217}At ($t_{1/2}$ = 32.3 ms; 7.1 MeV α particle), ^{213}Bi ($t_{1/2}$ = 45.6 min; 5.9 MeV α particle, 492 keV β^- particle and 440 keV γ emission), ^{213}Po ($t_{1/2}$ = 3.72 μs; 8.4 MeV α particle), ^{209}Tl ($t_{1/2}$ = 2.2 min; 178 keV β^- particle), ^{209}Pb ($t_{1/2}$ = 3.23 h; 198 keV β^- particle) and ^{209}Bi (stable). From this, a single ^{225}Ac decay yields a total of four α, three β^- disintegrations, and two γ emissions, which classifies ^{225}Ac as a "nanogenerator" or "in vivo generator". Therefore, the 9.9 d half-life of ^{225}Ac, the multiple α particle emissions in its decay chain, and its rapid decay to ^{209}Bi make ^{225}Ac an attractive candidate for TAT [21]. The γ emissions would be useful for SPECT imaging of in vivo radiopharmaceutical distribution, giving the ^{225}Ac decay series theranostic potential; however, due to the potency of ^{225}Ac, the small administered doses and correspondingly low γ emissions would make planar SPECT imaging difficult [21]. Of note, the intermediate ^{213}Bi possesses attractive potential and can be separated from the ^{225}Ac decay series for use. However, the short 45.6 min half-life of ^{213}Bi presents challenges for processing, radiolabeling, and radiopharmaceutical administration, resulting in a limited time in circulation to accumulate at its target site and achieve its intended therapeutic effects.

^{224}Ra ($t_{1/2}$ = 3.63 d, 5.7 MeV α particle, 241 keV γ emission) decays to ^{208}Pb with six intermediate radionuclide progenies. These daughters include ^{220}Rn ($t_{1/2}$ = 55.6 s, 6.3 MeV α particle), ^{216}Po ($t_{1/2}$ = 0.15 s, 6.8 MeV α particle), ^{212}Pb ($t_{1/2}$ = 10.6 h, 93.5 keV β^- particle, 238 keV γ emission), ^{212}Bi ($t_{1/2}$ = 60.6 min, 6.1 MeV α particle, 834 keV β^- particle, 727 keV γ emission), ^{212}Po ($t_{1/2}$ = 0.30 μs, 8.8 MeV α particle), ^{208}Tl ($t_{1/2}$ = 3.1 min, 650 keV β^- particle, 2614 keV γ emission), and ^{208}Pb (stable). From this, a single ^{224}Ra decay yields a total of four α particles, two β^- disintegrations, and six γ emissions, also classifying ^{224}Ra as a "nanogenerator". The bone-seeking properties of ^{224}Ra and its favorable half-life has resulted in its use in α-therapy, and its intermediates ^{212}Pb and ^{212}Bi show potential for TAT, with ^{212}Pb preferable to ^{212}Bi for administration due to the longer half-life of ^{212}Pb, permitting more dose from its ^{212}Bi progeny to be delivered [1].

^{227}Th ($t_{1/2}$ = 18.7 d, 6.0 MeV α particle, 236 keV γ emission) decays to ^{207}Pb with six intermediate radionuclide progenies. These daughters include ^{223}Ra ($t_{1/2}$ = 11.4 d, 5.7 MeV α particle, and 269 keV γ emission), ^{219}Rn ($t_{1/2}$ = 3.96 s, 6.8 MeV α particle, 271 keV γ emission), ^{215}Po ($t_{1/2}$ = 1.78 ms, 7.4 MeV α particle), ^{211}Pb ($t_{1/2}$ = 36.1 min, 471 keV β^- particle, 404 keV γ emission), ^{211}Bi ($t_{1/2}$ = 2.14 min, 6.6 MeV α particle, 172 keV β^- particle, 351 keV γ emission), ^{207}Tl ($t_{1/2}$ = 4.77 min, 492 keV β^- particle), and ^{207}Pb (stable). ^{227}Th and ^{223}Ra are both nanogenerators, releasing up to four α particles during the decay chain, and their γ emissions allow for imaging [1].

^{211}At ($t_{1/2}$ = 7.2 h, 5.9 MeV α particle) decays to ^{207}Pb with two intermediate radionuclide progenies in separate paths. These daughters include ^{207}Bi ($t_{1/2}$ = 31.6 y, electron capture) which decays to ^{207}Pb and ^{211}Po ($t_{1/2}$ = 0.52 s, 7.5 MeV α particle, Kα x-rays) which decays to ^{207}Pb. The decay to ^{211}Po would permit in vivo imaging of ^{211}At using the emitted Kα x-rays.

^{149}Tb ($t_{1/2}$ = 4.1 h, 4.0 MeV α particle, 638 keV β^+ particle), decays to ^{149}Sm and ^{145}Nd in two separate paths. In one path, its daughters include ^{149}G ($t_{1/2}$ = 9.28 d), ^{149}Eu ($t_{1/2}$ = 93.1 d, electron capture), and ^{149}Sm (stable). The other path includes ^{145}Eu ($t_{1/2}$ = 5.9 d, 740 keV β^+ particle, 894 keV γ emission), ^{145}Sm ($t_{1/2}$ = 340.3 d, electron capture, 61 keV γ emission), ^{145}Pm ($t_{1/2}$ = 17.7 y, electron capture, 72 keV γ emission), and ^{145}Nd (stable) [22]. The decay scheme for ^{149}Tb

is quite favorable since it releases short-range α particles from only one radionuclide, with complementary γ emissions and positrons that can be employed for imaging purposes in an “alpha-PET” combination [23][24]. Having only one α-emitter in its decay scheme implies a minimal toxicity from daughter recoil during radioactive decay, which should reduce excessive dose burden [25].

References

1. Poty, S.; Francesconi, L.C.; McDevitt, M.R.; Morris, M.J.; Lewis, J.S. α-Emitters for radiotherapy: From basic radiochemistry to clinical studies—Part 1. Nucl. Med. 2018, 59, 878–884, doi:10.2967/jnumed.116.186338.
2. Yeong, C.H.; Cheng, M.-H.; Ng, K.H. Therapeutic radionuclides in nuclear medicine: Current and future prospects. Zhejiang Univ. Sci. B 2014, 15, 845–863, doi:10.1631/jzus.b1400131.
3. Poty, S.; Francesconi, L.C.; McDevitt, M.R.; Morris, M.J.; Lewis, J.S. α-Emitters for radiotherapy: From basic radiochemistry to clinical studies—Part 2. Nucl. Med. 2018, 59, 1020–1027, doi:10.2967/jnumed.117.204651.
4. Sollini, M.; Marzo, K.; Chiti, A.; Kirienko, M. The five “W”s and “How” of targeted alpha therapy: Why? Who? What? Where? When? and How? Fis. Acc. Lincei 2020, 31, 231–247.
5. Ku, A.; Facca, V.J.; Cai, Z.; Reilly, R.M. Auger electrons for cancer therapy—A review. EJNMMI Radiopharm. Chem. 2019, 4, 1–36, doi:10.1186/s41181-019-0075-2.
6. Elgqvist, J.; Frost, S.; Pouget, J.-P.; Albertsson, P. The potential and hurdles of targeted alpha therapy—Clinical trials and beyond. Oncol. 2014, 3, 324, doi:10.3389/fonc.2013.00324.
7. Emmett, L.; Willowson, K.; Violet, J.; Shin, J.; Blanksby, A.; Lee, J. Lutetium177PSMA radionuclide therapy for men with prostate cancer: A review of the current literature and discussion of practical aspects of therapy. Med. Radiat. Sci. 2017, 64, 52–60, doi:10.1002/jmrs.227.
8. Das, S.; Al-Toubah, T.; El-Haddad, G.; Strosberg, J. 177Lu-DOTATATE for the treatment of gastroenteropancreatic neuroendocrine tumors. Expert Rev. Gastroenterol. Hepatol. 2019, 13, 1023–1031, doi:10.1080/17474124.2019.1685381.
9. Kassis, A.I. Molecular and cellular radiobiological effects of Auger emitting radionuclides. Prot. Dosim. 2010, 143, 241–247, doi:10.1093/rpd/ncq385.
10. Capello, A.; Krenning, E.; Bernard, B.; Reubi, J.-C.; Breeman, W.; de Jong, M. 111In-labelled somatostatin analogues in a rat tumour model: Somatostatin receptor status and effects of peptide receptor radionuclide therapy. J. Nucl. Med. Mol. Imaging 2005, 32, 1288–1295, doi:10.1007/s00259-005-1877-x.
11. Li, L.; Quang, T.S.; Gracely, E.J.; Kim, J.H.; Emrich, J.G.; Yaeger, T.E.; Jenrette, J.M.; Cohen, S.C.; Black, P.; Brady, L.W. A phase II study of anti–epidermal growth factor receptor radioimmunotherapy in the treatment of glioblastoma multiforme. Neurosurg. 2010, 113, 192–198, doi:10.3171/2010.2.jns091211.
12. Neshasteh-Riz, A.; Mairs, R.J.; Angerson, W.J.; Stanton, P.D.; Reeves, J.R.; Rampling, R.; Owens, J.; Wheldon, T.E. Differential cytotoxicity of [123I]IUdR, [125I]IUdR and [131I]IUdR to human glioma cells in monolayer or spheroid culture: Effect of proliferative heterogeneity and radiation cross-fire. J Cancer 1998, 77, 385–390.
13. Humm, J.L.; Cobb, L.M. Nonuniformity of tumor dose in radioimmunotherapy. Nucl. Med. 1990, 31, 75–83.
14. Nikula, T.K.; McDevitt, M.R.; Finn, R.D.; Wu, C.; Kozak, R.W.; Garmestani, K.; Brechbiel, M.W.; Curcio, M.J.; Pippin, C.G.; Tiffany-Jones, L.; et al. Alpha-emitting bismuth cyclohexylbenzyl DTPA constructs of recombinant humanized anti-CD33 antibodies: Pharmacokinetics, bioactivity, toxicity and chemistry. Nucl. Med. 1999, 40, 166–176.
15. Dong, Z.; Tan, Z.; Chen, P.; Schneider, N.; Glover, S.; Cui, L.; Torgue, J.; Rixe, O.; Spitz, H.B. Significant systemic therapeutic effects of high-LET immunoradiation by 212Pb-trastuzumab against prostatic tumors of androgen-independent human prostate cancer in mice. J. Oncol. 2012, 40, 1881–1888, doi:10.3892/ijo.2012.1357.
16. Kratochwil, C.; Bruchertseifer, F.; Giesel, F.L.; Weis, M.; Verburg, F.A.; Mottaghy, F.; Kopka, K.; Apostolidis, C.; Haberkorn, U.; Morgenstern, A. 225Ac-PSMA-617 for PSMA-targeted α-radiation therapy of metastatic castration-resistant prostate cancer. Nucl. Med. 2016, 57, 1941–1944.
17. Chan, H.S.; Konijnenberg, M.W.; Daniels, T.; Nysus, M.V.; Makvandi, M.; De Blois, E.; Breeman, W.A.P.; Atcher, R.W.; de Jong, M.; Norenberg, J.P. Improved safety and efficacy of 213Bi-DOTATATE-targeted alpha therapy of somatostatin receptor-expressing neuroendocrine tumors in mice pre-treated with l-lysine. EJNMMI Res. 2016, 6, 1–11, doi:10.1186/s13550-016-0240-5.
18. Chan, H.S.; de Blois, E.; Morgenstern, A.; Bruchertseifer, F.; de Jong, M.; Breeman, W.; Konijnenberg, M. In vitro comparison of 213Bi- and 177Lu-radiation for peptide receptor radionuclide therapy. PLoS ONE 2017, 12, e0181473,

doi:10.1371/journal.pone.0181473.

19. Kozempel, J.; Mokhodoeva, O.; Vlk, M. Progress in targeted alpha-particle therapy. What we learned about recoils release from in vivo generators. Molecules 2018, 23, 581, doi:10.3390/molecules23030581.
20. Sonzogni, A.; Shu, B. Nudat 2.8 (Nuclear Structure and Decay Data). 2020. Available online: Nndc.bnl.gov (accessed on 8 September 2020).
21. Scheinberg, D.A. Actinium-225 in targeted alpha-particle therapeutic applications. Radiopharm. 2011, 4, 306–320, doi:10.2174/1874471011104040306.
22. Wood, V.; Ackerman, N.L. Cherenkov light production from the α-emitting decay chains of 223Ra, 212Pb, and 149Tb for cherenkov luminescence imaging. Radiat. Isot. 2016, 118, 354–360, doi:10.1016/j.apradiso.2016.10.009.
23. Allen, B.J.; Blagojevic, N. Alpha- and beta-emitting radiolanthanides in targeted cancer therapy: The potential role of terbium-149. Med. Commun. 1996, 17, 40–47.
24. Müller, C.; A Domnanich, K.; A Umbricht, C.; Van Der Meulen, N.P. Scandium and terbium radionuclides for radiotheranostics: Current state of development towards clinical application. J. Radiol. 2018, 91, 20180074, doi:10.1259/bjr.20180074.
25. Moiseeva, A.N.; Aliev, R.A.; Unezhev, V.N.; Zagryadskiy, V.A.; Latushkin, S.T.; Aksenov, N.V.; Gustova, N.S.; Voronuk, M.G.; Starodub, G.Y.; Ogloblin, A.A. Cross section measurements of 151Eu(3He,5n) reaction: New opportunities for medical alpha emitter 149Tb production. Rep. 2020, 10, 1–7, doi:10.1038/s41598-020-57436-6.